# COMMERCIAL APPLICATIONS MULTISPECTRAL SENSOR SYSTEM

**Ronald J. Birk**
**Sverdrup Technology**
**Stennis Space Center, MS 39529**

**Bruce Spiering**
**NASA Science and Technology Laboratory**
**Stennis Space Center, MS 39529**



## ABSTRACT

NASA's Office of Commercial Programs is funding a multispectral sensor system to be used in the development of remote sensing applications. The Airborne Terrestrial Applications Sensor (ATLAS) is designed to provide versatility in acquiring spectral and spatial information. The ATLAS system will be a test bed for the development of specifications for airborne and spaceborne remote sensing instrumentation for dedicated applications. This objective requires spectral coverage from the visible through thermal infrared wavelengths, variable spatial resolution from 2-25 meters; high geometric and geo-location accuracy; on-board radiometric calibration; digital recording; and optimized performance for minimized cost, size, and weight. ATLAS is scheduled to be available in 3rd quarter 1992 for acquisition of data for applications such as environmental monitoring, facilities management, geographic information systems data base development, and mineral exploration.

## 1. BACKGROUND

The NASA Office of Commercial Programs (OCP) has a key cooperative effort with US industry to enhance our nation's economic standing in space-based remote sensing technology[1]. OCP's Commercial Earth Observations Program (CEOP) is designed to increase US economic returns from remote sensing and related spatial information services. OCP provided Stennis Space Center (SSC) with mission requirements (Table I) for engineering and support of a versatile sensor system for developing remote sensing applications.

Table I Mission Requirements

| | |
|---|---|
| (M1) | Provide prototype sensor system and subsystem test, verification, and applications proof-of-concept. |
| (M2) | Provide a flexible configuration for determining optimal sensor system design for specific applications to facilitate subsequent scanner development with private funds. |
| (M3) | Provide for calibration of other aircraft or satellite sensor systems during concurrent data acquisition missions. |
| (M4) | Utilize advanced and/or innovative technologies to decrease the cost and complexity of a remote sensing system, while attempting to increase the capability and end-user functionality of the data. |

Stennis Space Center (SSC) acts as the lead center for remote sensing for OCP. SSC has operated an airborne multispectral data acquisition facility since 1972. The Thematic Mapper Simulator (TMS), Daedalus Enterprises[a]

[a] Mention of products/companies does not imply endorsement by the US Government, NASA, or Lockheed Engineering & Sciences Company. References are provided solely for the benefit of the reader.

developed Thermal Infrared Multispectral Scanner[2] (TIMS) and the Calibrated Airborne Multispectral Scanner (CAMS) have successfully supported 590 missions across the United States, Canada and Central America. These missions were predominately sponsored by NASA and other government agency earth resource monitoring projects. Although these sensors have some attributes to support commercial applications development, they are limited by the following:

- o Priority use to support science research projects.
- o System specifications designed to support science applications.
- o Configurations not conducive to spectral or spatial resolution modifications.
- o System/subsystem design based on > 5 year old technology.

Specifications for the ATLAS system were developed through an analysis of viable designs. These designs were based on functional requirements[3] (Table II) derived from the mission requirements stated above and for compatibility with existing aircraft and on-going commercial programs at SSC.

Table II ATLAS Functional Requirements

| | |
|---|---|
| (F1) | Deployable from a Learjet 23 or compatible aircraft. |
| (F2) | Airborne and satellite-based sensor system emulation. |
| (F3) | Multispectral response from the visible through thermal infrared (0.4 - 12.5$\mu$m) wavelengths. |
| (F4) | Ground spatial resolution ranging from 2-25 meters, with design emphasis on less than 10 meters. |
| (F5) | Reflective and emissive calibration sources traceable to national standards. |
| (F6) | Modular and reconfigurable system subassemblies. |
| (F7) | Accurate aircraft attitude and geo-location knowledge to provide ancillary data for high geometric fidelity. |
| (F8) | Direct digital recording. |
| (F9) | High reliability, ease of maintainability, and operator interface optimization. |

## 2. INTRODUCTION

This paper provides a functional description (Section 3) and performance parameters (Section 4) of the ATLAS system that is currently under development. Results of analysis[4] to determine the system signal-to-noise ratio (SNR), noise equivalent radiance (NER) and noise equivalent temperature differential (NE$\Delta$T) were calculated with a sensor analysis software package. The program is called Analytical Tools for Thermal Infrared Engineering (ATTIRE)[5] and was developed at Stennis. Other system parameters include positioning accuracy, geometric fidelity, and digital recorder interface specifications. The technical specifications are listed in Appendix 6.2.

ATLAS (Figure 1) is an opto/mechanical scanner with multi-channel detector modules. ATLAS is designed to acquire data in 15 discrete channels in 5 atmospheric windows of the 0.4 - 12.5 $\mu$m region of the electromagnetic spectrum. The system has 3 spectrometers referred to as: visible/near infrared (VNIR), shortwave/midwave infrared (SW/MWIR), and the thermal infrared (TIR). Simultaneous acquisition of data in is of significant value in evaluating optimal sensor system performance for a particular application. Channel center wavelength and

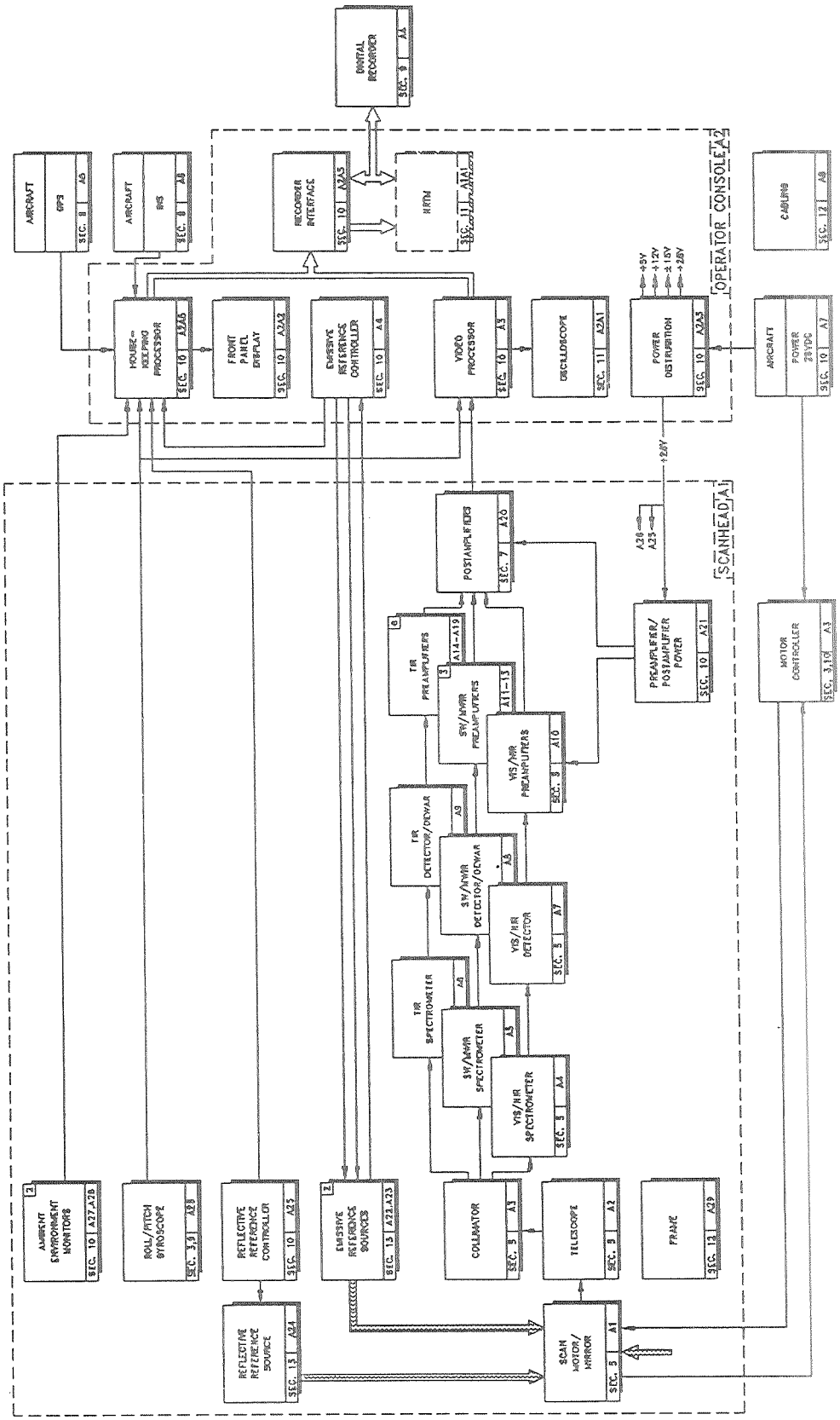


Figure 1 - Sensor System Block Diagram

bandwidth can be varied by changing modular spectrometers and/or detector assemblies.

Design of a visible through thermal infrared sensor system requires a detailed analysis of input signal propagation through the system. The major components in developing a model for the sensor system are the source, atmosphere, optics, detector, spatial parameters, and preamplifier electronics. The final goal of the analysis is to determine the performance parameters of SNR, NER, and NEΔT for each channel. The atmospheric interference for each spectral bandpass is modeled with the PC version of LOWTRAN 7 and results are incorporated in the ATTIRE modeling of SNR, NER, and NEΔT.

## 3. ATLAS SYSTEM

The ATLAS system consists of a scan head to be mounted in the equipment bay of the Learjet 23 aircraft and the operator console that is rack mounted in the cabin. The scan head (Figure 2) houses the scan motor/mirror assembly, telescope, 3 spectrometers, detector assemblies, calibration sources, and preamplifier electronics. The operator console includes the video processing electronics, ancillary data (housekeeping) control electronics, blackbody and motor controllers, and monitoring instrumentation.

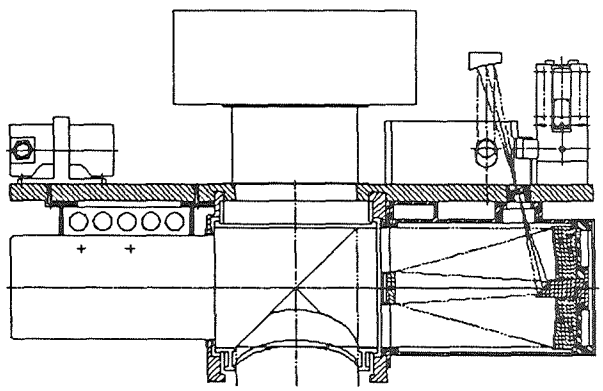

Figure 2 Scan Head Schematic

### 3.1 Spatial Parameters

Spatial resolution is determined by aircraft altitude, velocity and scan speed. ATTIRE utilizes the relationship expressed in Equation 1 to determine scan speed effects on performance. An airborne platform capable of flying at altitudes between 1000 and 14,000 meters in altitude allows for sensor spatial ground resolution to be varied from 2-25 meters. The system has a variable integration time as a function of scan speed. To acquire 2 meter ground resolution, an aircraft velocity of 195 knots at an altitude of 1000 meters is required at a scan speed of 50 rps.

$$GIFOV = \alpha\, a = \frac{v}{n} \tag{1}$$

where GIFOV = ground spatial resolution (meters); n = scan speed
a = altitude of aircraft (meters); v = aircraft velocity (m/s)
$\alpha$ = angular IFOV

Distortions are introduced in the spatial data as a function of the scanning configuration (Figure 3). Examples include widening of pixels at the scan edges and the "S" effect due to the forward motion of the plane during a flight line and aircraft dynamics. These distortions may be corrected during post-processing with appropriate compensation data.

### 3.2 Optics

The optics subsystem collects, focuses, and disperses the radiant flux from the source to 3 spectrometers. The energy is then focused onto individual detectors. The two parameters that are critical to the collection of this energy are the area of the entrance aperture of the optics and the focal length. The radiance, limited by the solid angle subtended by the ground pixel, is incident on the entrance aperture and determines the irradiance available to the optics.

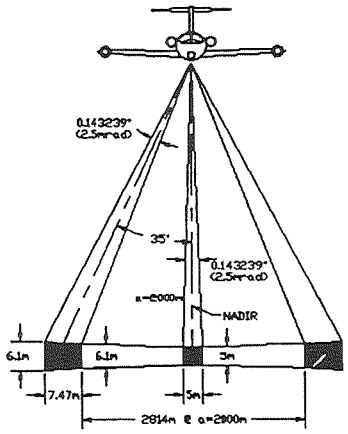


Figure 3 - Pixel Size Variation

The telescope and the 3 spectrometers were designed at SSC[6] using Optical Research Associates (ORA) Code V optical design software. The telescope is a 7.5" aperture Dall-Kirkham design with an f-number of 7.84 and a 2 mrad field stop. Ground radiation is reflected by the scan mirror onto the telescope primary mirror. The converging radiation is reflected from the primary onto the secondary mirror, then to a folding flat mirror. The radiation is focused off-axis onto a square field stop aperture that defines the 2 mrad instantaneous field of view (IFOV) for the system. Above the field stop, an optical window is mounted to seal the spectrometer assembly from the atmosphere.

The TIR spectrometer uses a collimating and a folding mirror to direct the incoming radiation to a dichroic filter that separates the 8.2-12.2 $\mu$m radiation from the shorter wavelengths (0.45-4.2 $\mu$m). The transmitted radiation is dispersed into 6 channels by a reflective grating, and then focused onto a HgCdTe detector array using an achromatic objective. The objective is a germanium triplet of 40 mm diameter, with an effective focal length (EFL) of 25.5 mm and a back focal length (BFL) of 20.5 mm. The objective is well corrected over the 8-12 $\mu$m region and is ideally suited for this compact spectrometer.

The SW/MWIR spectrometer accepts the reflected radiation from the TIR dichroic filter and separates the 1.55-4.2 $\mu$m energy from the visible (0.45-0.90 $\mu$m) radiation using a second dichroic filter. The transmitted radiation is dispersed into 3 channels by a reflective grating onto an InSb detector array using an achromatic objective. The objective is a ZnS-Si-ZnS triplet that is 38 mm in diameter with an EFL of 32.5 mm and a BFL of 17.5 mm.

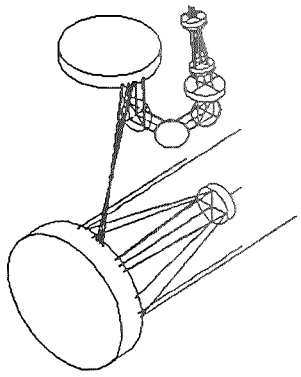

**Figure 4** VNIR Spectrometer & Telescope

The VNIR spectrometer (Figure 4) disperses radiation between 0.45-0.90 $\mu$m into 6 channels. The VNIR radiation is separated from the longer wavelength energy by reflection from the second dichroic filter. A transmission grating with a groove spacing of 300 lines/mm is used to disperse the collimated radiation to a pair of achromatic doublets that focus the dispersed light onto the silicon detector array. The doublets are standard off-the-shelf achromats.

### 3.3 Detectors

The detectors were chosen based on performance in each spectral region. A 6 element silicon array will be used for the 6 VNIR channels. An indium/antimonide (InSb) array incorporated in a $LN_2$ dewar assembly will be used for the 3 SW/MWIR channels. A mercury cadmium telluide (HgCdTe) array incorporated in a $LN_2$ dewar assembly will be used for the 6 thermal channels.

### 3.4 Preamplifiers

The VNIR and SW/MWIR channels using photovoltaic (PV) detectors with a high impedance ($>$ 500 M$\Omega$) will use preamplifiers operated in an unbiased mode to take advantage of the characteristic high $D^*$ value. The TIR channels using photoconductive (PC) detectors with low impedance (20-120$\Omega$) will have preamplifiers configured in a Wheatstone bridge circuit.

The gain requirements for each channel depend on the input signal from the detectors. The photovoltaic detector amplifiers will deliver a gain between $10^6$ and $10^7$. The photoconductive detector amplifiers will have an average gain of 200-300. Bandwidth requirements for the amplifiers are established by the maximum scan speed of 50 rps. Therefore, the electronic bandwidth, $\Delta f$, must have a minimum value of 79.54 kHz.

## 3.5 Video Processor

The major functions of the video processor are signal conditioning, anti-alias filtering, analog-to-digital conversion (ADC), and buffering. The analog signal from the postamplifiers on the scan head will be routed through fiber optic cable for EMI/RFI noise suppression to the operator console in the cabin. Gain and offset controls will be used by the operator to optimize dynamic range. Sufficient gain is applied to the signal to obtain a maximum amplitude of 10V p-p. The analysis to determine the digitization resolution resulted in a requirement of $>10$ bits. To meet this requirement, a 12 bit Datel Inc. analog-to-digital convertor with integral sample and hold was chosen.

## 3.6 Timing

The position of the mirror is critical for precise timing of video sampling. The encoder resolution of the motor/mirror assembly is 4096 pulses per revolution, or 1.53 mrad. From this a master clock with a frequency of 12.5x the encoder frequency is generated. A timing diagram of the sampling sequence is shown in Figure 5.

## 3.7 Housekeeping

The housekeeping subsystem interface architecture (Figure 6) is designed to incorporate the ancillary data required during post-processing and provide other system functions such as roll compensation. Interfaces to the aircraft inertial navigation system (INS), global positioning system (GPS) receiver, blackbody controller, scan head gyroscope, ambient temperature sensors, front panel controls, real-time clock, mission specific data, and input for system calibration parameters are required. These functions are implemented through a dual microcontroller-based "embedded control" design. The microcontroller chosen was a Motorola 68HC11 running at a machine cycle of 0.5 $\mu$s.

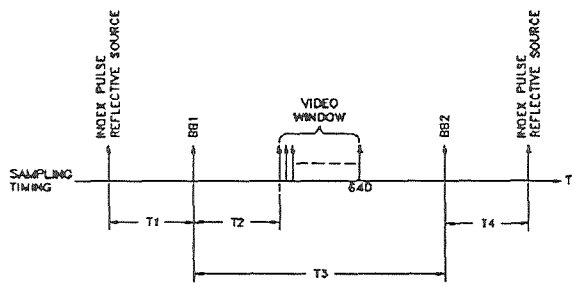


Figure 5 - Sampling Timing

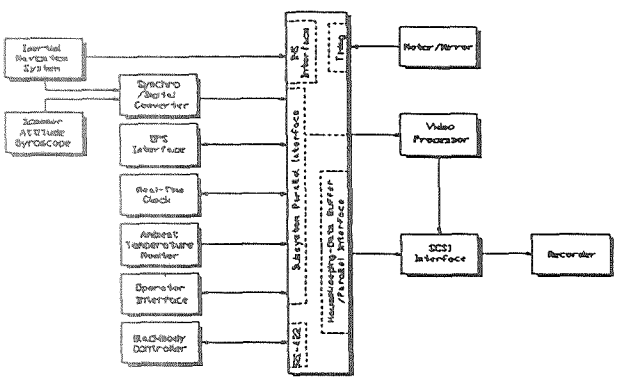


Figure 6 Subsystem Interface Architecture

### 3.7.1 Global Positioning System Interface

Geo-location knowledge is important for maximizing the usefulness of remotely sensed data. This is particularly true when the data are intended to be incorporated into a geographic information system (GIS). Accurate location knowledge is necessary for coregistering remotely sensed data sets to perform change detection analysis.

The ATLAS Global Positioning System (GPS) receiver will be a differential unit. Position, velocity, and time (PVT) is calculated at a 1-2Hz rate and is precisely time tagged to allow synchronization of the GPS signals with systems that are tied to it. The total number of satellites in the GPS constellation will be 21 plus 3 active spares by 1994. The GPS constellation now consists of 13 satellites and provides world-wide 2-D coverage, with 3-D coverage in "windows" (times when four or more satellites are in view). An 18-satellite constellation will provide global 3-D positioning, and is expected sometime in 1992. The full constellation, in conjunction with differential operation, will allow for positional uncertainties of $\leq 5$ meters in latitude, longitude, and altitude.

A comparison of the accuracies of the aircraft inertial navigation system (INS) (values are taken at the equator) and differential GPS under best case conditions is presented in Table III. Two-dimensional (latitude and longitude) positional errors translate directly to the ground scene (assuming straight and level flight). A 5 meter lat/long

Table III GPS versus INS Accuracy

| | LAT (m) | LONG (m) | ALT (m) | TIME (s) | DRIFT (°) | GND SP (knts) |
|---|---|---|---|---|---|---|
| INS | 177 | 177 | N/A | 0.1 | 1 | 1 |
| GPS | 5 | 5 | 5 | 1e-9 | N/A | 0.3 |

circular error translates to 1 pixel for a 2 mrad system at an altitude of 4,125 feet. At an altitude of 41,250 feet, accuracies of 1/10 pixel are possible.

Geometric fidelity is a fundamental requirement of many applications of remotely sensed imagery. For airborne and spaceborne systems, geometric distortion is introduced in the imagery as a function of platform dynamics. An airborne scanner is subject to dynamic motion in roll, pitch, yaw, altitude, and velocity vectors which interact in a complex manner. Correction by manual intervention with standard processing techniques is time consuming and yields results with limited accuracy. Information provided by the GPS and system roll/pitch gyro provide for computer-assisted rectification of the data.

3.7.2 Roll/Pitch Gyroscope

A roll/pitch gyroscope is mounted directly on the scan head to minimize rotational error due to misalignment between the gyroscope and scan head. The outputs of the gyroscope are 3-wire synchro outputs that can be sampled continuously and are synchronized to the ATLAS system. The output of the aircraft INS gyro is also recorded.

The output is converted to a 14 bit digital number using two synchro-to-digital converters (SDC). Values for roll and pitch are stored in housekeeping. Roll output is used for real-time roll correction. The typical angular error for the gyroscope is $< \pm 0.2°$ from true pitch and roll angles over full scale. This equates to $\pm 1.75$ pixels at nadir for a 2.0-mrad system and represents the accuracy to which the gyroscope can locate the nadir pixel. It is a constant offset and once determined can be subtracted from all pitch and roll values. The angular repeatability is typically $\pm 0.05°$ or less and is equivalent to $\pm 0.44$ pixel. With the inclusion of quantization error, the angular error is within $\pm 1.93$ pixels and the angular repeatability is within $\pm 0.92$ pixel.

## 3.8 Digital Recorder

Recording of data using compact digital technology meets the mission requirement of implementing new technology to increase capability while decreasing cost. The 8 mm helical scan Exabyte digital recorder technology can handle most data rates generated by the ATLAS. The Exabyte 8500 recorder has a 5 Gbyte per tape capacity and a throughput of 0.5 Mbytes per second. Two units will handle 15 channels of 12 bit data at maximum scan speed. By designing the system to format the data to be compatible with image processing software and using a tape drive that complies to a standard computer interface (SCSI), data can be read directly into an image processing workstation upon delivery by the aircraft data acquisition crew. The 8 mm recorders are lighter ($<50$ lb) and smaller ($<600$ in$^3$) than conventional wide-band analog units and have significantly lower procurement and operating costs. They eliminate the requirement for a decommutation system, which represents a savings of around $1M in support hardware and software.

## 3.9 Operator Interface

The operator interface performs 4 basic functions:

- o Provide for operator control of system power, channel gain and offset adjustment, blackbody set points, scan speed, tape recorder, and oscilloscope.
- o Data entry of mission number, time, date and performance parameters.

- o Provide indicators of system operation and performance of dynamic range, noise, parameter values, image quality.
- o Conduct and monitor diagnostic tests.

The operator console is ergonomically designed for access to controls on the oscilloscope for monitoring analog, digital, and recorded signals. Provisions have been made to incorporate a near-real-time monitor (NRTM) to display video data in flight.

### 3.10 Calibration Sources

Radiometric calibration is required for performing quantitative data analysis. For a system that operates in both the reflective and emissive regions of the spectrum, calibrated reflective (lamp) and emissive (blackbody) reference sources, whose calibration is traceable to national standards, are required. The reflective source has been designed as a modified integrated sphere available from Labsphere, Inc. The blackbody sources were designed at SSC and manufactured by Mikron Industries.

## 4. SENSOR SYSTEM PERFORMANCE

ATLAS performance parameters (Table IV) were determined for each channel assuming a standard solar curve[7,8] for the reflective channels, with an albedo of 0.3, and a 300°K blackbody curve for the emissive channels. The average values for atmospheric transmission from sea level to a nominal altitude of 7000 meters were determined from Lowtran 7 and tables from Hudson[9]. Optical transmission was determined for each channel through analysis in Code V optical design software and vendor transmission and reflection curves for individual optical components. The effective focal length varies for each channel; values are listed in Table IV. Detector $D^*$, was obtained from vendor test data and input as 3e13 for the VNIR, 2.41e11 for the SW/MWIR, and 4.46e10 for the TIR. Preamplifier noise factor, $n_f$, determined in laboratory tests at SSC, was input as 1.2 and preamplifier bandwidth as set at 78.5 KHz. Scan speed was taken to be 25 rps, providing a dwell time of 12.73 $\mu$seconds. The system performance parameters of SNR, NER, and NE$\Delta$T were calculated using the ATTIRE system analysis modeling software. Results of the modelling of the system design using actual data that characterizes the subsystems indicates very good performance. NER for the visible channels is much less than 0.5% and NE$\Delta$T for the thermal channels is on the order of 0.2°C. A summary of the radiometric equations used to calculate the performance parameters is provided in Appendix 6.1. Technical specifications for the ATLAS system are presented in Appendix 6.2.

## 5. CONCLUSIONS

The ATLAS system will be accessible through Stennis Space Center for industry to use as a test bed for the investigation of potential remote sensing applications. Optimal spatial and spectral specifications can be determined through the acquisition of coincident spectral coverage over a range of ground resolutions. Specifications for a support a particular application can then be provided to commercial sensor manufacturers for production. This program is designed to facilitate the use of remote sensing technology to acquire information exceeding the current capabilities of the Landsat and SPOT sensor systems.

The sensor system will provide good image quality performance, high geometric fidelity, and direct sensor-to-computer interface through digital recording media. Commercial users have priority use of the ATLAS system to develop the use of remote sensing technology for applications such as environmental monitoring, facilities management, geographic information systems data base development, and mineral exploration.

**Table IV** ATLAS Performance Parameters

| CH | Band Limit ($\mu$m) | Source (W $cm_{-2}$ $sr_{-1}$) | Atm ($\tau_a$) | Optics ($\tau_o$) | EFL (cm) | SNR (dB) | NER (%) | NE$\Delta$T (°C) |
|---|---|---|---|---|---|---|---|---|
| 1 | 0.45-0.52 | 3.31e-4 | 0.60 | 0.17 | 61.0 | 92 | 0.0025 | N/A |
| 2 | 0.52-0.60 | 6.80e-4 | 0.60 | 0.30 | 64.5 | 98 | 0.0013 | N/A |
| 3 | 0.60-0.63 | 2.52e-4 | 0.60 | 0.30 | 39.4 | 93 | 0.0021 | N/A |
| 4 | 0.63-0.69 | 4.97e-4 | 0.60 | 0.30 | 56.0 | 96 | 0.0015 | N/A |
| 5 | 0.69-0.76 | 3.76e-4 | 0.60 | 0.24 | 60.5 | 93 | 0.0022 | N/A |
| 6 | 0.76-0.90 | 3.95e-4 | 0.60 | 0.20 | 89.8 | 90 | 0.0031 | N/A |
| 7 | 1.55-1.75 | 2.79e-4 | 0.80 | 0.35 | 36.0 | 35 | 0.5765 | N/A |
| 8 | 2.08-2.35 | 1.69e-4 | 0.80 | 0.32 | 40.4 | 30 | 1.0642 | N/A |
| 9 | 3.35-4.20 | 2.01e-3 | 0.80 | 0.13 | 66.4 | 47 | 0.458 | 0.118 |
| 10 | 8.20-8.60 | 3.99e-4 | 0.75 | 0.42 | 21.0 | 43 | 0.7327 | 0.19 |
| 11 | 8.60-9.00 | 4.69e-4 | 0.75 | 0.48 | 21.0 | 44 | 0.6234 | 0.16 |
| 12 | 9.00-9.40 | 5.07e-4 | 0.75 | 0.51 | 21.0 | 45 | 0.5775 | 0.15 |
| 13 | 9.60-10.2 | 7.04e-4 | 0.75 | 0.47 | 26.0 | 46 | 0.5151 | 0.14 |
| 14 | 10.2-11.2 | 9.51e-4 | 0.75 | 0.39 | 34.7 | 46 | 0.5089 | 0.13 |
| 15 | 11.2-12.2 | 5.29e-4 | 0.75 | 0.23 | 34.7 | 41 | 0.9142 | 0.24 |

## 6. APPENDICES

### 6.1 Radiometric Performance Analysis

This appendix presents calculations[9,10] performed to determine SNR, NER, and NE$\Delta$T for a channel of the ATLAS system .

#### 6.1.1 Source Bandpass Flux

The bandpass flux exiting from the source pixel is calculated by

$$L_e(\lambda,T) = \int_{\lambda_1}^{\lambda_2} \frac{\epsilon(\lambda)}{\pi} \frac{c_1}{\lambda^5 \left(\exp(c_2/\lambda T) - 1\right)} d\lambda \quad W\,cm^{-2}sr^{-1} \tag{2}$$

where $\epsilon(\lambda)$ = spectral emissivity
$\lambda_1$ = lower wavelength of the channel
$\lambda_2$ = upper wavelength of the channel.

### 6.1.2 Bandpass Flux Incident on the Detector

This radiance propagates through the atmosphere and the optical path of the sensor system before it is incident on the detector. The radiance incident on the detector is thus attenuated by the atmospheric and optical transmittance, and can be calculated by

$$L_e^d(T) = \tau_a \tau_o L_e(T) \quad W\ cm^{-2}\ sr^{-1} \tag{3}$$

where $\tau_a$ = atmospheric transmittance
$\tau_o$ = optical transmittance

### 6.1.3 Throughput/Power Incident on the Detector

The radiance incident on the detector multiplied by the throughput ($\Upsilon$) of the system yields the power incident on the detector. The throughput is defined as the product of the area of the detector and the solid angle subtended by the detector towards the imaging lens. By the Invariance of Throughput Theorem, this throughput also equals the product of the pixel area and solid angle subtended to the collecting lens.

$$\Upsilon = A_{pix}\Omega_e = A_d\Omega_l \quad cm^2\ sr \tag{4}$$

where $A_{pix}$ = Area of ground pixel
$A_d$ = Area of detector
$\Omega_e$ = Solid angle subtended by ground pixel at entrance aperture
$\Omega_l$ = Solid angle subtended by detector at the imaging lens
imaging lens

### 6.1.4 Noise Equivalent Power (NEP)

Noise Equivalent Power is defined as the power incident on the detector such that the SNR is unity. Using $D^*_{bb}$, detector area, and electrical bandwidth, the NEP can be determined by

$$NEP(T) = \frac{\sqrt{A_d\ \Delta f}}{D^*_{bb}(T_B)} \quad W \tag{5}$$

where $A_d$ = Area of the detector
$\Delta f$ = electronic bandwidth
$D_{bb}$ = $D^*$ normalized to blackbody temperature

### 6.1.5 Signal-to-Noise Ratio (SNR)

An expression for the SNR of the signal from the detector may be obtained from the NEP calculation

$$SNR_d = \frac{P_d}{NEP(T)} \tag{6}$$

where $P_d$ = Power to the detector

### 6.1.6 Noise Equivalent Radiance (NER)

NER is defined as radiance incident on the sensor that produces an SNR of unity. At the detector output, NER is

$$NER_d = \frac{L_e^{BB}(T)}{SNR_d} \quad W\ cm^{-2}\ sr^{-1} \tag{7}$$

6.1.7 Noise Equivalent Temperature Difference (NEΔT)

Noise Equivalent Temperature Difference is defined as the change in target temperature that produces an SNR of unity. The following is an expression for NEΔT

$$NE\Delta T = \frac{n_f}{\frac{P_d}{\sqrt{A_d \Delta f}} \frac{D^*(\lambda_{pk})}{\lambda_{pk}} \frac{C_2}{T^2}} \ ^\circ K \tag{8}$$

where $C_2$ = hc/k = 1.44e-4 $\mu$m K

## 6.2 Specifications Summary

**Table V** ATLAS Technical Specifications

| Optical | | Geometric | |
|---|---|---|---|
| Entrance aperture | 7.5" | GPS accuracy | 5 meters |
| F-number (VNIR/SWIR/TIR) | 2.46/1.2/0.95 | INS accuracy | 177 meters (at the equator) |
| Spatial | | Gyroscope accuracy | 0.05° |
| TFOV | 73.34° | Roll correction | ±15° |
| IFOV | 2 mrad | Electronic | |
| Scan speed | 6-50 rps | Digitization resolution | 12 bits |
| Calibration Sources | | Analog bandwidth | DC-78.54 kHz |
| Field Filling | 100% | Video words | 640/channel |
| Uniformity | >95% | Housekeeping words | 200 |
| Stability | >95% | Recorder | |
| Emissivity (thermal) | 0.99 | Throughput | 0.8 Mbytes/s |
| Settability (thermal) | 0.1°C | Storage Capacity | >2 Gbytes/tape |
| Accuracy (thermal) | 0.1°C | Interface | SCSI |
| Weight | 435# | Power | 22-32 VDC @ 74 A |

## 7. ACKNOWLEDGEMENTS

This study was performed for the Commercial Earth Observations Program at Stennis Space Center for the NASA Office of Commercial Programs. The authors wish to thank the engineering staff of the Advanced Sensor Development Laboratory for their outstanding work on the development of this sensor system and their contributions to this paper.

## 8. REFERENCES

1. Birk, R.J., Tompkins, J.M., and Burns, G.S. (1991) "Commercial remote sensing small satellite feasibility study," *SPIE Vol. 1495 Small Satellite Technology and Applications*, pp 2-12.

2. Palluconi, F., Meeks, G. (1985) "Thermal Infrared Multispectral Scanner (TIMS): An Investigator's Guide to TIMS Data," *JPL Publication 85-32.*

3. Birk, R.J., Christensen, E., and Alexander, T. (1991) "Airborne Instrument Testbed System (AITS) Strategic Plan," *Internal Report* (Contact R. Birk at Stennis Space Center for a copy).

4. ASDL Engineering (1991) "ATLAS System Analysis," *Internal Report*, (Contact Bruce Spiering at Stennis Space Center for a copy).

5. Jaggi, S. (1991) "ATTIRE (Analytical Tools for Thermal Infrared Engineering)," *Proceedings of the Second Annual JPL Airborne Geoscience Workshop.*

6. DaMommio, A. and Kuo, S. (1992) "Optical design for the ATLAS multispectral scanner," *SPIE Vol. 1690 Design of Optical Instruments* (Submitted for publication).

7. Thekaekara, M.P., Kruger,T., and R. Duncun (1962) "Solar Irradiance Measurements from a Research Aircraft," *Applied Optics*, Vol. 8 No. 8, pp 1713-1732.

8. Moon, P. (1940) "Proposed Standard Solar-Radiation Curves for Engineering Use," *J. Franklin Inst.*, Vol. 230, No. 5 pp 583-617.

9. Wyatt, C. (1987) Radiometric System Design, MacMillian Publishing Company, New York.

10. Hudson, R. (1969) Infrared System Engineering, John Wiley & Sons, New York.